

# The Reinvigoration of the Southern Ocean Carbon Sink

Peter Landschützer<sup>1\*</sup>, Nicolas Gruber<sup>1,2</sup>, F. Alexander Haumann<sup>1,2</sup>,  
Christian Rödenbeck<sup>3</sup>, Dorothee C.E. Bakker<sup>4</sup>, Steven van Heuven<sup>5,6</sup>,  
Mario Hoppema<sup>5</sup>, Nicolas Metzl<sup>7</sup>, Colm Sweeney<sup>8</sup>, Taro Takahashi<sup>9</sup>,  
Bronte Tilbrook<sup>10</sup> & Rik Wanninkhof<sup>11</sup>

<sup>1</sup>Environmental Physics, Institute of Biogeochemistry and Pollutant Dynamics,  
ETH Zürich, Zürich, Switzerland,

<sup>2</sup>Center for Climate Systems Modeling, C2SM, ETH Zürich, Zürich, Switzerland,

<sup>3</sup>Max Planck Institute for Biogeochemistry, Jena, Germany,

<sup>4</sup>Centre for Ocean and Atmospheric Sciences, School of Environmental Sciences,  
University of East Anglia, Norwich, UK,

<sup>5</sup>Alfred Wegener Institute Helmholtz Centre for Polar and Marine Research,  
Bremerhaven, Germany,

<sup>6</sup>now at Dept. of Marine Geology and Chemical Oceanography,  
Royal Netherlands Institute of Sea Research (NIOZ), Texel, The Netherlands

<sup>7</sup>Sorbonne Universités (UPMC, Univ Paris 06)-CNRS-IRD-MNHN,  
LOCEAN/IPSL Laboratory, 4 place Jussieu, F-75005 Paris, France,

<sup>8</sup>NOAA Earth System Research Laboratory, Boulder, Colorado, USA,

<sup>9</sup>Lamont-Doherty Earth Observatory of Columbia University, Palisades, USA,

<sup>10</sup>Commonwealth Scientific and Industrial Research Organisation (CSIRO) and Antarctic  
Climate and Ecosystems Co-operative Research Centre, Hobart, Australia,

<sup>11</sup>Atlantic Oceanographic and Meteorological Laboratory (AOML) of NOAA, Miami, USA

\*E-mail: peter.landschuetzer@usys.ethz.ch.

**Several studies have suggested that the carbon sink in the Southern Ocean - the ocean's strongest region for uptake of anthropogenic CO<sub>2</sub> - has weakened in recent decades. Here, we demonstrate on the basis of multi-decadal analyses**

**of surface ocean CO<sub>2</sub> observations that this weakening trend stopped around 2002 and that by 2012, the Southern Ocean had regained its expected strength based on the growth of atmospheric CO<sub>2</sub>. All three Southern Ocean sectors have contributed to this reinvigoration of the carbon sink, yet differences in the processes between sectors exist, related to a tendency towards a zonally more asymmetric atmospheric circulation. The large decadal variations in the Southern Ocean carbon sink suggest a rather dynamic ocean carbon cycle that varies more in time than previously recognized.**

Simulations with ocean biogeochemical models have suggested a stagnation or even a reduction of the Southern Ocean carbon sink from the 1980s to the early-2000s (1–3), a result that has been supported by inversion studies (1) based on atmospheric CO<sub>2</sub> data. Such a stagnation has wide-reaching implications to climate as the Southern Ocean south of 35°S accounts for about 40% of the global oceanic uptake of anthropogenic CO<sub>2</sub> (4–6), thereby contributing a disproportionately large share in the removal of anthropogenic CO<sub>2</sub> from the atmosphere. The trend towards a saturation of the Southern Ocean carbon sink has been attributed mainly to the intensification and poleward shift of the westerly winds associated with a trend towards a more positive state of the Southern Annular Mode (1, 2). The resulting enhanced upwelling of deep waters with high concentrations of dissolved inorganic carbon (DIC) drove an anomalously strong flux of natural CO<sub>2</sub> out of the surface ocean, counteracting the increase in the oceanic uptake of anthropogenic CO<sub>2</sub> (2).

Several studies based on observations of the surface partial pressure of CO<sub>2</sub> (7–9) corroborated these model-based trends in the Southern Ocean carbon sink, but all of them used the observations without any interpolation. Given the sparsity and spatial heterogeneity of these surface ocean observations (8), the conclusions drawn in these studies regarding the trends turn out to be rather sensitive to the chosen method of trend calculation (9) and the beginning and

end year of analysis (10). Nevertheless, these studies tended to support a weakening sink trend up to the mid 2000s. One of these studies (9) also pointed out that the trend may have reversed in recent years, a finding corroborated by the analysis of  $p\text{CO}_2$  observations along a single meridional transect south of Tasmania (11).

To address the sparse data coverage, we use a neural network technique (12) to interpolate the  $p\text{CO}_2$  observations in time and space. We then evaluate the results using (i) a complementary  $p\text{CO}_2$  observation-based product based on the interpolation by a data-driven mixed layer scheme (13), and (ii) an atmospheric  $\text{CO}_2$  inverse estimate (14). Both surface ocean based methods have been extended for this study to produce multi-decadal distributions of the surface ocean  $p\text{CO}_2$  field (15, 16). The air-sea  $\text{CO}_2$  flux variations are then computed employing a standard bulk parameterization (see supplement 1.4). Though each of these estimates faces limits due to the available information, their combination allows us to gain confidence in the inferred features.

The two surface ocean data-based air-sea  $\text{CO}_2$  flux products confirm that the Southern Ocean carbon sink (south of  $35^\circ\text{S}$ ) weakened through much of the 1990s, in agreement with the model-based studies and the atmospheric inversions (1, 2), but reveal that it has strengthened substantially since about 2002, increasing by more than  $\sim 0.6 \text{ Pg C yr}^{-1}$  (see Fig. 1) to a vigorous uptake of  $\sim 1.2 \text{ Pg C yr}^{-1}$  in 2011. This increase has returned the Southern Ocean sink to levels expected from the increase in atmospheric  $\text{CO}_2$  (5), computed from an ocean biogeochemistry model forced with just the increase in atmospheric  $\text{CO}_2$  (17). The increase in the Southern Ocean carbon uptake since 2002 is responsible for roughly half of the global trend in the ocean carbon sink over this period (15), highlighting the importance of the Southern Ocean in moderating the growth of atmospheric  $\text{CO}_2$ .

Both surface ocean observation based methods rely on the to-date largest sea surface  $p\text{CO}_2$  observation database (SOCAT version 2) (18), which contains more than 2.6 million observations in the Southern Ocean south of  $35^\circ\text{S}$ . The neural network technique (12, 15) interpolates

these observations to a  $1^\circ \times 1^\circ$  global grid at a monthly resolution for the period 1982 through 2011, resulting in a multi-decadal reconstruction of the global ocean carbon sink. The method relies on non-linear but robust relations between the limited  $p\text{CO}_2$  observations and properties measured more frequently such as sea-surface temperature, sea-surface salinity, satellite chlorophyll-a and mixed layer depth (see supplement 1.2). The mixed layer scheme (13, 16) (version oc\_v1.2) in contrast does not regress  $p\text{CO}_2$  variations to physical, chemical or biological driver data, but directly assimilates the available  $p\text{CO}_2$  observations into a mass-budget of the mixed layer at a resolution of  $4^\circ \times 5^\circ$  in space and daily in time. This method also uses several ancillary observations to parameterize the air-sea  $\text{CO}_2$  exchange, solubility and carbon chemistry, but does not use them to interpolate the  $p\text{CO}_2$  to regions without observations. Instead, it interpolates the  $p\text{CO}_2$  data directly.

Extensive validation of the neural network based estimate using independent observations reveal that the method is able to map the sparse  $p\text{CO}_2$  data with little bias (mean differences between SOCAT observations and neural network estimates of generally less than  $2 \mu\text{atm}$ ; see Table S1) in space and time. Both methods agree well regarding the sign and the magnitude of the decadal trends within the two decades from 1992 through 2001 and 2002 through 2011 (Fig. 1, Table S2), where the majority of surface ocean  $p\text{CO}_2$  observations exist (Fig. S3).

However, given the methodological differences in the data treatment in data-sparse regions (interpolation versus regression), there is less agreement regarding higher frequency variability such as the year-to-year variations in the sink strength. This lower agreement is a result of the weaker signal-to-noise ratio of the  $p\text{CO}_2$  data in the interannual frequency band. Under such conditions, the direct interpolation scheme of the mixed layer method tends to extrapolate high-frequency noise present in the observations to the data sparse region, likely generating overly strong variations there. In contrast, the neural network scheme suppresses the high-frequency noise by being constrained by the ancillary observations, resulting in a possible underestimation

of the year-to-year variability in the data-sparse regions. In contrast, the relatively strong  $p\text{CO}_2$  signals that underlie the decadal changes in the Southern Ocean are distinctly captured by the two methods, resulting in very similar decadal trends.

The changes in the Southern Ocean carbon sink are almost entirely driven by changes in the air-sea difference of  $p\text{CO}_2$ , i.e.,  $\Delta p\text{CO}_2 = p\text{CO}_2^{\text{sea}} - p\text{CO}_2^{\text{atm}}$  ( $p\text{CO}_2^{\text{atm}} = \text{atmospheric } p\text{CO}_2$ ), since the direct effect of changes in the wind and temperature on the gas transfer coefficient is small (see Fig. S8). The spatial pattern of the trends in  $\Delta p\text{CO}_2$  from the neural network method reveals for both decades a very uniform trend pattern across the entire Southern Ocean, with the strongest  $\Delta p\text{CO}_2$  trends at high latitudes (see Fig. 2a& b). The spatial trends for the mixed layer scheme are similar, although at coarser resolution and with somewhat more zonal variations, part of which may be spurious due to missing data constraints there, reflecting the more variance producing nature of this method in data-sparse regions (see Fig. S6). From 1992 through 2001, the trend in  $\Delta p\text{CO}_2$  was strongly positive, driven by the surface ocean  $p\text{CO}_2$  increasing nearly twice the rate of  $p\text{CO}_2^{\text{atm}}$  around Antarctica. In contrast, from 2002 onward, the growth of surface ocean  $p\text{CO}_2$  nearly stalled, strongly increasing the degree of surface ocean undersaturation, which ultimately drove the increasing uptake of atmospheric  $\text{CO}_2$ .

We test the robustness of this result on the basis that such strong decadal changes in the  $\text{CO}_2$  uptake across most of the Southern Ocean should leave an imprint on atmospheric  $\text{CO}_2$ , taking advantage of the lack of land regions with substantial  $\text{CO}_2$  fluxes south of  $35^\circ\text{S}$ . Specifically, we are using an atmospheric inversion method (14) to infer the air-sea  $\text{CO}_2$  fluxes that are optimally consistent with the atmospheric  $\text{CO}_2$  data while taking into consideration atmospheric transport and mixing. The employed setup that is the same as the published version s85\_v3.6, but we used the atmospheric winds from ERA-Interim reanalysis (19). The evolution of the Southern Ocean carbon sink from this inversion of atmospheric  $\text{CO}_2$  data also supports our postulated larger than expected increase in the Southern Ocean carbon sink strength within the last decade

(Fig. 1), even though it shows much less of a weakening during the 1990s. In conclusion, two complementary  $p\text{CO}_2$  data based estimates, as well as an atmospheric  $\text{CO}_2$  inversion confirm that the Southern Ocean carbon sink experienced a significant strengthening since the early 2000s.

This reinvigoration after the early 2000s cannot be a simple reversal of the Southern Annular Mode-driven wind trend that has been suggested to cause the weakening of the Southern Ocean carbon sink over the past decades (1, 2), because the ERA-Interim reanalysis winds (19) do not show such a signal (Fig. 2g-h). Instead, the atmospheric circulation became more zonally asymmetric with a wave-number two pattern, reminiscent of the lower frequency pattern of variability of the Antarctic Circumpolar Wave (20). But how can this zonally asymmetric forcing result in a relatively zonally uniform response of the surface ocean  $p\text{CO}_2$ ?

Insight into the drivers is gained by separating the  $\Delta p\text{CO}_2$  trend pattern into a component driven by changes in sea-surface temperature (i.e., thermal trend; Fig. 2c and Fig. 2e), and one driven by changes in the dissolved inorganic carbon (DIC) and/or alkalinity (i.e., non-thermal trend; Fig. 2d and Fig. 2f) (21). For both analysis periods, the trends in the thermal and non-thermal components are generally opposed for any given location, in line with previous studies (21–23). The thermal component shows a sink increase in both decades in the Pacific sector, where the advection of cold air from Antarctica and sea-ice changes led to a persistent surface cooling trend (24). In the lower latitudes of the Atlantic and Indian sectors, we find a reduced thermally-driven uptake in the 2000s due to surface ocean warming, which is probably related to the more asymmetric atmospheric circulation that caused a reduced northward Ekman transport (Fig. S11) of cold polar waters in these regions.

In the non-thermal component, we find more distinct differences between the two periods. Between 1992 and 2001, the non-thermal component increased the oceanic  $p\text{CO}_2$  over most of the Southern Ocean (Fig. 2d), in particular in the high latitudes and in the Pacific sector. The

estimated changes in Ekman pumping velocity (estimated from ERA-Interim winds (19), Fig. S11) support the hypothesis that wind changes led to an increased surface divergence and an associated upwelling of DIC-rich waters into all sectors of the high-latitude Southern Ocean (2) in the first period. During the subsequent period, the non-thermal component primarily reduced the oceanic  $p\text{CO}_2$  in the Atlantic and Indian sectors and over the Antarctic shelf (Fig. 2f). In contrast, this component continued to increase  $p\text{CO}_2$  in most of the Pacific sector, though at a much weaker rate than in the 1990s. This much weaker DIC and/or alkalinity induced increase in  $p\text{CO}_2$  in the Pacific sector could no longer compensate for the thermal trend, so that the negative trend in the total  $p\text{CO}_2$  in this region for the period after 2001 is dominated by the thermal trend. In contrast, in the Atlantic, Indian sector, and over the Antarctic shelf, the negative non-thermal trend dominates the thermal changes. Thus, overall, the temperature dominated  $p\text{CO}_2$  trend in the Pacific sector, and the DIC/alkalinity-driven trend in the other regions worked in tandem to prevent the  $p\text{CO}_2$  to increase across the entire Southern Ocean since the early 2000s. Over the same period, atmospheric  $\text{CO}_2$  continued to rise strongly, resulting in a substantial increase of the undersaturation of the surface ocean with regard to atmospheric  $\text{CO}_2$ , hence driving a strong increase in the flux of  $\text{CO}_2$  into the entire Southern Ocean.

We interpret this zonal asymmetry of thermal- and DIC-/alkalinity-driven changes to be primarily the result of an increased asymmetry in the southern hemisphere atmospheric circulation in the years since 2001 (Fig. 3). Specifically, the conditions became more cyclonically dominant in the Pacific sector, and more anti-cyclonically dominant in the Atlantic and parts of the Indian sector (Fig. 2h). As a result of the associated increase in the meridional wind components, more cold air was advected from the Antarctic continent over the Pacific sector, and more warm air was advected from subtropical latitudes over the Atlantic and part of the Indian sectors. Together with the changes in northward Ekman transport (Fig. S11), this provides an explanation for the strengthened asymmetry in the sea-surface temperature trends, which

underlie the thermal trends in Fig. 2e.

A strengthening of the carbon sink in the Pacific sector combined with the further intensification of the winds (Fig. 2h) during the 2000s provide a paradox at first sight, since the increased upwelling in the Pacific sector should have increased the surface DIC content further. A possible explanation is that the recent stabilization of the surface waters (25) counteracted the wind induced upwelling. In the Pacific sector and in coastal regions, strong surface freshening (25, 26) might have caused most of this stabilization, while in the lower latitudes of the Atlantic and Indian sector warming stabilized the surface waters. The reduction in northward Ekman transport to the lower latitude Atlantic and Indian sector during the 2000s (Fig. S11), that is probably the result of the zonally more asymmetric atmospheric circulation, also reduced the northward advection of high-latitude waters, lowering the DIC content and/or increasing the alkalinity at the surface.

The trend towards a zonally more asymmetric atmospheric circulation may be related to long-term variations of the tropical sea-surface temperature, i.e., to the more prevalent La Niña conditions in the Pacific since the early 2000s (27) and the more positive phase of the Atlantic Multidecadal Oscillation over recent decades (28). Alternatively, it may be driven by a zonally asymmetric response of the southern hemisphere near-surface circulation to the anthropogenic forcing (24).

Our results indicate that Earth's most important sink for anthropogenic CO<sub>2</sub> (5, 6) is more variable than previously suggested, and that it responds quite sensitively to physical climate variability. This also suggests, that should current climate trends reverse in the near future, the Southern Ocean might lose its recently regained uptake strength, leading to a faster accumulation of CO<sub>2</sub> in the atmosphere and consequently an acceleration of the rate of global warming.

## References and Notes

1. C. Le Quéré, *et al.*, *Science* **316**, 1735 (2007).
2. N. S. Lovenduski, N. Gruber, *Global Biochemical Cycles* **22**, GB3016 (2008).
3. A. Lenton, *et al.*, *Biogeosciences* **10**, 4037 (2013).
4. C. L. Sabine, *et al.*, *Science (New York, N.Y.)* **305**, 367 (2004).
5. S. E. Mikaloff Fletcher, *et al.*, *Global Biogeochemical Cycles* **20**, GB2002 (2006).
6. T. L. Frölicher, *et al.*, *Journal of Climate* **28**, 862 (2015).
7. N. Metzl, *Deep Sea Research Part II: Topical Studies in Oceanography* **56**, 607 (2009).
8. T. Takahashi, *et al.*, *Oceanography* **25(3)**, 26 (2012).
9. A. R. Fay, G. A. McKinley, N. S. Lovenduski, *Geophysical Research Letters* **41**, 6833 (2014).
10. N. S. Lovenduski, A. R. Fay, G. A. McKinley, *Global Biogeochem. Cycles* **28** (2015).
11. L. Xue, L. Gao, W.-J. Cai, W. Yu, M. Wei, *Geophysical Research Letters* **42**, 3973 (2015).
12. P. Landschützer, *et al.*, *Biogeosciences* **10**, 7793 (2013).
13. C. Rödenbeck, *et al.*, *Ocean Science* **9**, 93 (2013).
14. C. Rödenbeck, S. Houweling, M. Gloor, M. Heimann, *Atmos. Chem. Phys.* **3**, 1919 (2003).
15. P. Landschützer, N. Gruber, D. C. E. Bakker, U. Schuster, *Global Biogeochemical Cycles* **28**, 927949 (2014).
16. C. Rödenbeck, *et al.*, *Biogeosciences* **11**, 4599 (2014).

17. H. D. Graven, N. Gruber, R. Key, S. Khatiwala, X. Giraud, *J. Geophys. Res.* **117**, C10005 (2012).
18. D. C. E. Bakker, *et al.*, *Earth System Science Data* **6**, 69 (2014).
19. D. P. Dee, *et al.*, *Quarterly Journal of the Royal Meteorological Society* **137(656)**, 553 (2011).
20. A. F. Carril, A. Navarra, *Geophysical Research Letters* **28**, 4623 (2001).
21. T. Takahashi, *et al.*, *Deep-Sea Research II* **49**, 1601 (2002).
22. N. Gruber, *et al.*, *Global Biogeochemical Cycles* **23**, GB1005 (2009).
23. J. D. Majkut, J. L. Sarmiento, K. B. Rodgers, *Global Biogeochemical Cycles* **28**, 335 (2014).
24. F. A. Haumann, D. Notz, H. Schmidt, *Geophysical Research Letters* **41**, 8429 (2014).
25. C. De Lavergne, J. B. Palter, E. D. Galbraith, R. Bernardello, I. Marinov, *Nature Climate Change* **4**, 278 (2014).
26. S. S. Jacobs, C. F. Giulivi, *Journal of Climate* **23**, 4508 (2010).
27. E. J. Ding, Q. and. Steig, D. S. Battisti, M. Kittel, *Nature Geosciences* **4**, 398 (2011).
28. X. Li, D. M. Holland, E. P. Gerber, C. Yoo, *Nature* **505**, 538 (2014).

Acknowledgements: This work was supported by EU grant 264879 (CARBOCHANGE) (PL, NG, DCEB, MH, SVH, NM) and EU grant 283080 (GEO-CARBON) (PL, NG), both of which received funding from the European Commission's Seventh Framework Programme. FAH was supported by ETH research grant CH2-01 11-1. TT, RW and CS acknowledge funding for the  $p\text{CO}_2$  from ship projects from the Climate Observation Division of NOAA.

TT and the Ship of Opportunity Observation Program (SOOP) were supported by a grant (NA10OAR4320143) from the United States NOAA. CS contribution to this research was made possible by support from the U.S. National Science Foundation's Office of Polar Programs (AOAS 0944761 and AOAS 0636975). BT was funded through the Australian Climate Change Science Program and the Integrated Marine Observing System. CR thanks the providers of atmospheric CO<sub>2</sub> measurements, and the DKRZ computing center for their support. The Surface Ocean CO<sub>2</sub> Atlas (SOCAT) is an international effort, supported by the International Ocean Carbon Coordination Project (IOCCP), the Surface Ocean Lower Atmosphere Study (SOLAS), and the Integrated Marine Biogeochemistry and Ecosystem Research program (IMBER), to deliver a uniformly quality-controlled surface ocean CO<sub>2</sub> database. The many researchers and funding agencies responsible for the collection of data and quality control are thanked for their contributions to SOCAT. We also thank Andy Hogg for fruitful discussions. The surface ocean CO<sub>2</sub> observations are available from the SOCAT website ([www.socat.info](http://www.socat.info)). The surface ocean as well as atmospheric inverse flux dataset can be obtained upon request by contacting the corresponding author.

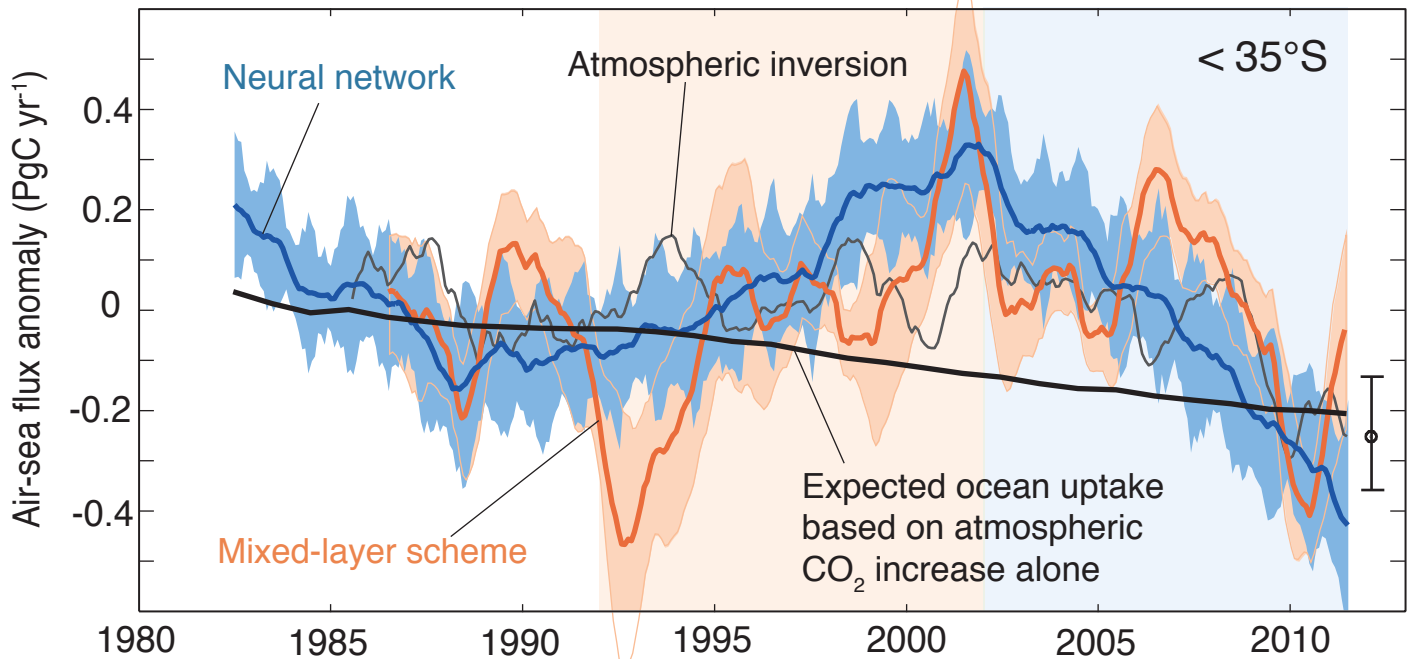
Contributions: PL and NG designed the study and wrote the paper together with FAH. PL developed the neural network estimation and performed the majority of the analyses, assisted by FAH. CR developed the mixed-layer scheme and the atmospheric inversion. SVH, MH, NM, CS, TT, BT and RW were responsible for the collection of the majority of the surface ocean CO<sub>2</sub> data in the Southern Ocean. DCEB led the SOCAT synthesis effort that underlies this work. All authors discussed the results and implications and commented on the manuscript at all stages.

**Fig. 1.** Evolution of the Southern Ocean carbon sink anomaly south of 35°S. The lines show the integrated air-sea CO<sub>2</sub> flux derived from two complementary surface ocean pCO<sub>2</sub> interpolation methods (a 2-step neural network technique (15) and a mixed layer scheme (16)) as well as the integrated flux from an atmospheric inversion based on measurements of atmospheric CO<sub>2</sub> (14). The horizontal error bar represents the uncertainty of the inverse estimate based on different realizations. These estimates are compared with the expected uptake based on the growth of atmospheric CO<sub>2</sub> alone, based on simulations with the ocean component of the Community Climate System Model (CCSM3) (17). All data are plotted as anomalies by subtracting the 1980-1990 mean flux from each method.

**Fig. 2.** Trends in  $\Delta p\text{CO}_2$  based on the neural network output and its two components for the two analysis decades, i.e., from 1992 through 2001 and from 2002 through 2011. (a) Linear trend in  $\Delta p\text{CO}_2$  for the 1990s; (b) as (a) but for the 2000s. Linear trend in (c) thermal pCO<sub>2</sub> and (d) non-thermal  $\Delta p\text{CO}_2$  for the 1990s; (e) and (f), as (c) and (d), but for the 2000s. Positive (red)  $\Delta p\text{CO}_2$  trends indicate a faster increase of pCO<sub>2</sub> in the surface ocean than in the atmosphere, i.e., a decreasing sink, and vice versa for positive (blue) trends. Hatched areas indicate where the linear trends are outside the 5% significance level ( $p \geq 0.05$ ). (g) and (h) illustrate decadal trends of sea level pressure (shading) and 10-m wind (vectors) from 1992 through 2001 (g) and 2002 through 2011 (h) based on data from ERA-Interim (19).

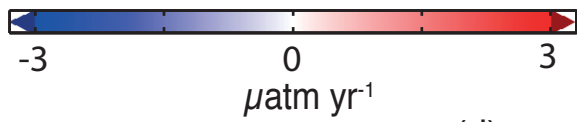
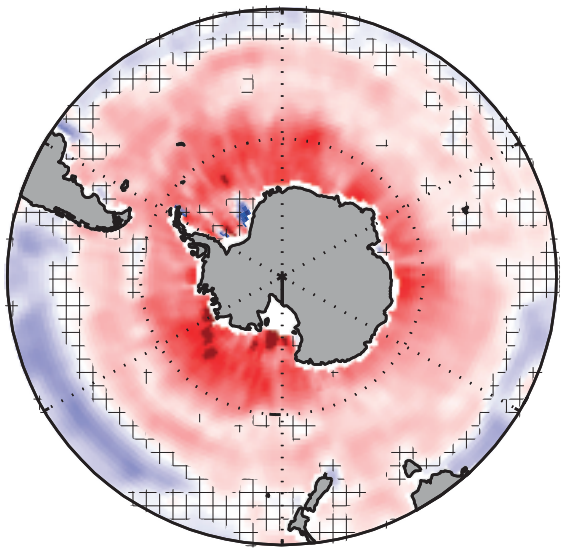
**Fig. 3.** Schematic of the processes governing the changes in the  $\Delta p\text{CO}_2$  trends in the Southern Ocean since 2001. The trend toward a zonally more asymmetric distribution of the atmospheric pressure systems in the last decade led to stronger meridional winds bringing either colder air (Pacific sector) or warmer air (Atlantic sector) to the open Southern Ocean, causing strong cooling of the sea surface in the Pacific sector and warming in the Atlantic sector. The changes in wind also affect the oceanic circulation pattern, with the net effect being a increase in the DIC/Alk driven pCO<sub>2</sub> component in the Pacific sector, and a decrease of this component in

the Atlantic sector, i.e., opposing the effect of sea surface temperature on  $p\text{CO}_2$ . In the Pacific sector, the effect of the cooling trend on  $p\text{CO}_2$  prevails, while in the Atlantic sector, the effect of circulation/mixing on DIC/Alk prevails, also causing a lowering trend in  $p\text{CO}_2$ . Thus, owing to the interaction between temperature and circulation changes, the zonally asymmetric forcing caused a zonally relatively symmetric response of the ocean carbon sink.



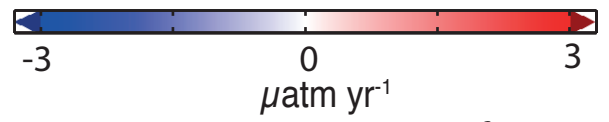
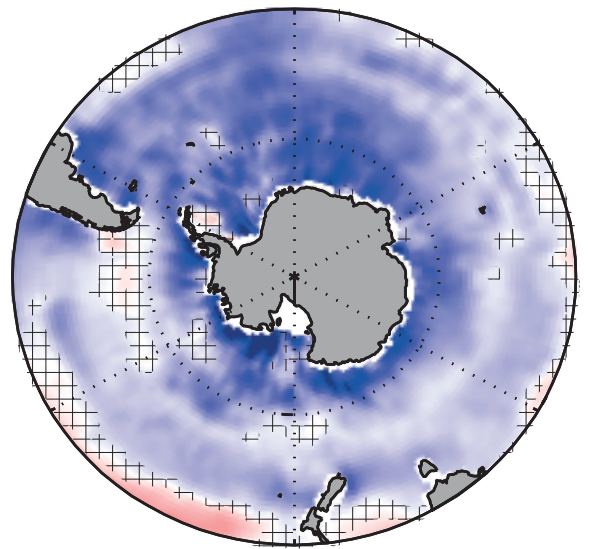
1992 - 2001

(a)



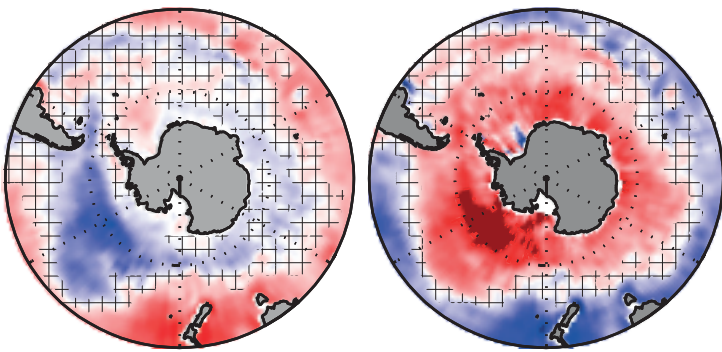
2002 - 2011

(b)



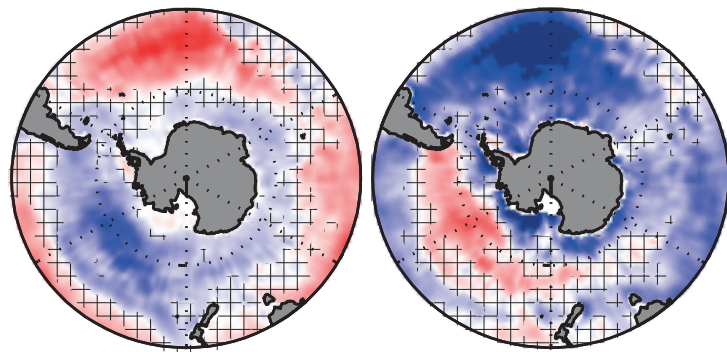
(c)

(d)



(e)

(f)



(g)

(h)

